

# A MATRIX COMPLETION APPROACH FOR WALL-CLUTTER MITIGATION IN COMPRESSIVE RADAR IMAGING OF INDOOR TARGETS

Van Ha Tang<sup>‡</sup> Abdesselam Bouzerdoum<sup>\*†</sup> Son Lam Phung<sup>\*</sup>

<sup>‡</sup>Faculty of Information Technology, Le Quy Don Technical University, Hanoi, Vietnam

<sup>\*</sup>School of Electrical, Computer and Telecommunications Engineering,  
University of Wollongong, Australia

<sup>†</sup>College of Science and Engineering, Hamad Bin Khalifa University, Doha, Qatar

## ABSTRACT

This paper presents a low-rank matrix completion approach to tackle the problem of wall clutter mitigation for through-wall radar imaging in the compressive sensing context. In particular, the task of wall clutter removal is reformulated as a matrix completion problem in which a low-rank matrix containing wall clutter is reconstructed from compressive measurements. The proposed model regularizes the low-rank prior of the wall-clutter matrix via the nuclear norm, casting the wall-clutter mitigation task as a nuclear-norm penalized least squares problem. To solve this optimization problem, an iterative algorithm based on the proximal gradient technique is introduced. Experiments on simulated full-wave electromagnetic data are conducted under compressive sensing scenarios. The results show that the proposed matrix completion approach is very effective at suppressing unwanted wall clutter and enhancing the targets.

**Index Terms**— Through-the-wall radar imaging, wall clutter mitigation, compressed sensing, low-rank matrix recovery, sparse reconstruction.

## 1. INTRODUCTION

Through-the-wall radar imaging (TWRI) has emerged as a useful technology for capturing scenes behind walls and other visually opaque materials. The ability to sense through enclosed structures has numerous civilian and military applications, such as search and rescue operations in environmental disasters and hidden hostage localizations in police missions [1–4]. Imaging indoor scenes, however, is difficult due to strong front-wall electromagnetic (EM) returns, which typically dominate the backscattered radar targets [5–7]. Hence, prior to image reconstruction, wall clutter mitigation needs to be performed for target detection and localization.

Early TWRI techniques for stationary targets [8–11] assume having the data collected from an empty scene without targets. The empty-scene data is used to subtract wall clutter. This approach is effective for clutter mitigation, but is infeasible in practice. Therefore, several techniques have been developed for wall clutter reduction without having recourse to an empty scene [5–7]. In [5], a spatial filtering (SF) technique was used for wall-clutter mitigation. This method considers the invariant property of the wall reflections and uses a notch filter for removing low spatial frequency signals containing wall contributions. In [6], a subspace projection (SP) method was developed to segregate the target returns from the wall reflections. The SP technique exploits the strength of wall reflections over that of the target signals. It applies singular value decomposition (SVD) to the radar signal matrix to estimate the wall subspace,

which is used for orthogonal projection to remove the wall reflections. In [7], a sparse Bayesian learning technique was proposed to determine the wall subspace from the received data adaptively. These approaches, however, are not suitable for compressive sensing (CS) operations; they consider only the full sensing mode and require full data measurements for effective wall clutter mitigation.

Recent approaches were proposed for enhanced TWRI using compressive sensing (CS) framework [12, 13]. It has been shown in [14–16] that CS allows a high-resolution scene reconstruction even if data measurements are reduced. Before using CS, wall clutter needs to be removed. However, because of missing measurements, existing wall clutter mitigation techniques are not as effective if applied directly to the compressed measurements. To overcome this issue, wall clutter alleviation in the CS context typically consists of two stages [14–17]: (i) antenna signal recovery and (ii) wall clutter suppression. Before using a wall clutter mitigation technique, the antenna signal recovery is performed using incomplete measurements. In other words, the two-stage clutter suppression technique alleviates the effects of wall reverberations by first estimating missing measurements and then applying a wall clutter mitigation method to the recovered data. However, they may face the issue of multi-stage uncertainties because the signal reconstruction and wall clutter suppression tasks are performed separately.

This paper introduces a low-rank matrix completion (LR-MC) approach for wall clutter mitigation in compressive TWR sensing. The proposed approach reformulates the problem of wall clutter mitigation as a regularized least squares (LS) optimization problem, where the objective function comprises an LS term and a nuclear-norm penalty term. The LS term measures the error bound, and the nuclear-norm term is a relaxed regularization for the low-rank property introduced over the wall-clutter matrix. Given the radar data matrix containing missing measurements, the goal is to estimate a rank-deficient matrix capturing the wall reflections. This paper proposes an iterative shrinkage algorithm, based on the proximal gradient technique to solve the optimization problem, yielding the clutter-free signals used for image reconstruction.

The remainder of the paper is organized as follows. Section 2 introduces the TWRI model. Section 3 presents the proposed LR-MC approach for clutter mitigation in CS TWRI. Section 4 presents experimental results. Section 5 gives concluding remarks.

## 2. THROUGH-WALL RADAR SIGNAL MODEL

This section presents briefly the signal model for a monostatic stepped-frequency radar system used to image targets situated in an indoor scene. The scene consisting of  $P$  targets is sensed by mov-

ing a transceiver parallel to the wall, synthesizing  $N$ -element array antenna. Each antenna transceives a stepped-frequency signal comprising  $M$  frequencies equispaced among the bandwidth. Let  $z_{m,n}$  denote the  $m$ -th frequency signal received by the  $n$ -th antenna. The signal  $z_{m,n}$  is modeled as the superposition of the wall reflection  $z_{m,n}^w$ , target return  $z_{m,n}^t$ , and noise  $v_{m,n}$ :

$$z_{m,n} = z_{m,n}^w + z_{m,n}^t + v_{m,n}. \quad (1)$$

The wall reflection  $z_{m,n}^w$  is given by

$$z_{m,n}^w = \sum_{r=1}^R \sigma_w a_r e^{-j2\pi f_m \tau_{n,w}^r}, \quad (2)$$

where  $R$  denotes the number of wall reverberations,  $\sigma_w$  is the reflectivity of the wall,  $a_r$  is the path loss factor of the  $r$ -th wall return, and  $\tau_{n,w}^r$  is the propagation delay of the  $r$ -th wall reverberation. The target signal is expressed as

$$z_{m,n}^t = \sum_{p=1}^P \sigma_p e^{-j2\pi f_m \tau_{n,p}}, \quad (3)$$

where  $\sigma_p$  is the reflectivity of the  $p$ -th target, and  $\tau_{n,p}$  is the signal travel time from the  $n$ -th antenna to the  $p$ -th target.

For image formation, the scene is divided into a rectangular grid consisting of  $Q$  pixels. Let  $s_q$  denote a weighted indicator function representing the  $p$ -th target reflectivity:

$$s_q = \begin{cases} \sigma_p, & \text{if the } p\text{-th target occupies the } q\text{-th pixel;} \\ 0, & \text{otherwise.} \end{cases} \quad (4)$$

Let  $\tau_{n,q}$  denote the focusing delay between the  $n$ -th antenna and the  $q$ -th pixel. Assuming the target comprising points located precisely on the image pixels, from (3) the target signal at the  $n$ -th antenna is expressed in matrix-vector form:

$$\mathbf{z}_n^t = \Psi_n \mathbf{s}, \quad (5)$$

where  $\mathbf{z}_n^t = [z_{1,n}^t, \dots, z_{M,n}^t]^T$ ,  $\Psi_n \in \mathbb{C}^{M \times Q}$  with the  $(m, q)$ -th entry given by  $\psi_n(m, q) = \exp(-j2\pi f_m \tau_{n,q})$ , and  $\mathbf{s} = [s_1, \dots, s_Q]^T$ . Stacking all measurements collected from the  $N$  antennas yields

$$\mathbf{z}^t = \Psi \mathbf{s}, \quad (6)$$

where  $\mathbf{z}^t = [(\mathbf{z}_1^t)^T, \dots, (\mathbf{z}_N^t)^T]^T$ , and  $\Psi = [\Psi_1^T, \dots, \Psi_N^T]^T$ .

From (6), the target image  $\mathbf{s}$  can be recovered from the target signal  $\mathbf{z}^t$  using CS technique or delay-and-sum (DS) beamforming. The CS technique promotes sparsity of the image  $\mathbf{s}$  and recovers it by solving an  $\ell_1$ -regularization problem. The DS beamforming method is only effective if full measurements are attained. Note that the target signal  $\mathbf{z}^t$  is unavailable in practice. Instead, we have only the radar signal  $\mathbf{z}$ , which is the target signal corrupted by the wall clutter  $\mathbf{z}^w$  and noise  $\mathbf{v}$ . Therefore, before image reconstruction, the target signal needs to be segregated from the wall clutter. Wall clutter mitigation techniques, such as SF [5] or SP [6], can be used if the same frequency measurements are available along the antennas. In general CS context, however, only a subset of frequency samples is collected, which may vary from one spatial position to another. To tackle this issue, two-stage wall clutter rejection approaches have been developed, where the missing measurements are first estimated, followed by wall clutter mitigation applied to the recovered measurements. The issue with the two-stage approach is that the performance is affected by the accuracy of the recovered signals. In this paper, the wall clutter removal task is formulated as a LR-MC problem, which is presented in the following sections.

### 3. LOW-RANK MATRIX COMPLETION TWRI

This section describes a LR-MC approach for clutter mitigation in CS TWRI. First, the received measurements along different antennas are represented in matrix-form. Then, the task of estimating the wall reflections is cast as a penalized LS minimization problem, where the nuclear-norm is enforced on the wall-clutter matrix. The formulation of the optimization problem is presented in the next subsection. Then, in Subsection 3.2, an algorithm is introduced for solving the minimization problem.

#### 3.1. Formulation of LR-MC problem

The radar signals received by all  $N$  antennas at  $M$  frequencies can be represented in matrix-form, as see Eq. 1,

$$\mathbf{Z} = \mathbf{Z}^w + \mathbf{Z}^t + \Upsilon, \quad (7)$$

where  $\mathbf{Z} = [z_{m,n}]$ ,  $\mathbf{Z}^w = [z_{m,n}^w]$ ,  $\mathbf{Z}^t = [z_{m,n}^t]$ , and  $\Upsilon = [v_{m,n}]$  denote the  $M \times N$  matrices containing, respectively, the antenna signals, the wall clutter, the target signals, and the noise.

In a compressed sensing TWRI scenario, we assume that only a reduced subset of  $K$  measurements ( $K \ll M \times N$ ) is acquired. Let  $\Phi \in \mathbb{R}^{K \times M \times N}$  denote a selection matrix. It has only one non-zero element (equal to 1) in each row indicating the selected frequency for a particular antenna. The measurement vector  $\mathbf{y} \in \mathbb{C}^K$  can be expressed as

$$\mathbf{y} = \Phi \text{vec}(\mathbf{Z}) = \mathcal{A}(\mathbf{Z}). \quad (8)$$

Here,  $\text{vec}(\mathbf{Z})$  denotes the vectorization operator stacking the columns of  $\mathbf{Z}$  into a composite column vector. Note that  $\mathbf{Z}$  can be obtained from  $\mathbf{y}$  as  $\mathbf{Z} = \text{mat}(\Phi^\dagger \mathbf{y}) = \mathcal{A}^*(\mathbf{y})$ , where  $\text{mat}$  denotes the operator reshaping a column vector of  $MN$  elements into an  $M \times N$  matrix, and  $\dagger$  is the pseudo-inverse operator.

Given the measurement vector  $\mathbf{y}$ , the aim is to recover the wall-clutter matrix  $\mathbf{Z}^w$ , exploiting its low-rank representation. The justification is in TWRI, the wall returns reside in a low-dimensional subspace [18, 19]. An estimate of  $\mathbf{Z}^w$  is obtained by solving the following MC problem:

$$\min_{\mathbf{Z}^w} \|\mathbf{Z}^w\|_* \quad \text{subject to} \quad \|\mathbf{y} - \mathcal{A}(\mathbf{Z}^w)\|_2^2 \leq \epsilon. \quad (9)$$

In (9),  $\|\mathbf{Z}^w\|_*$  denotes the nuclear-norm (the sum of the singular values of  $\mathbf{Z}^w$ , and  $\epsilon$  is a noise bound. The nuclear-norm regularization is the convex relaxation of rank minimization. Here, the condition for the recovery of low-rank matrix  $\mathbf{Z}^w$  is guaranteed because the entries of  $\Phi$  are random, and thus  $\mathcal{A}$  satisfies the restricted isometry property (RIP) constraint [20]. To solve Problem (9) efficiently, it can be cast into an unconstrained form or its Lagrangian version:

$$\min_{\mathbf{Z}^w} f(\mathbf{Z}^w) = \frac{1}{2} \|\mathbf{y} - \mathcal{A}(\mathbf{Z}^w)\|_2^2 + \gamma \|\mathbf{Z}^w\|_*, \quad (10)$$

where  $\gamma$  is a positive parameter. Convex analysis can be used to show the equivalence between of the solutions of (9) and (10). The next subsection introduces an iterative algorithm that can estimate the wall clutter  $\mathbf{Z}^w$  by minimizing  $f(\mathbf{Z}^w)$ .

#### 3.2. Iterative algorithm

This subsection describes an iterative algorithm to solve Problem (10). First, we consider the more generic case of minimizing a composite objective function:

$$\min_{\mathbf{x}} f(\mathbf{x}) = g(\mathbf{x}) + \gamma h(\mathbf{x}), \quad (11)$$

where  $g(\mathbf{x})$  is convex, differentiable, and smooth (the quadratic term in (10)) and  $h(\mathbf{x})$  is convex but not necessary smooth (the nuclear norm in (10)). This problem is solved efficiently using *proximal gradient technique*. Let  $\mathbf{x}_i$  be an estimate of the solution at the  $i$ -th iteration. Then, the next estimate of the minimizer is obtained by solving:

$$\mathbf{x}_{i+1} = \arg \min_{\mathbf{x}} \frac{1}{2} \|\mathbf{u}_i - \mathbf{x}\|_2^2 + \gamma \alpha h(\mathbf{x}), \quad (12)$$

where  $\mathbf{u}_i = \mathbf{x}_i - \alpha \nabla g(\mathbf{x}_i)$ . Here,  $\nabla g(\mathbf{x}_i)$  denotes the gradient of  $g(\mathbf{x})$  evaluated at the current estimate  $\mathbf{x}_i$ . When  $\nabla g$  is a Lipschitz continuous function with constant  $C$ , this method converges if  $\alpha \in (0, 1/C]$ . This generic optimization technique and its convergence guarantees have been widely used to solve the minimization problem (11) under different names: proximal gradient method [21], thresholded Landweber iteration [22], iterative shrinkage/thresholding [23], or separable approximation [24].

Here we use the iterative technique (12) to solve the problem in (10), i.e., minimizing  $f(\mathbf{Z}^w)$ . Let  $\mathbf{Z}_i^w$  denote an estimate of the solution at the  $i$ -th iteration. The next estimate is obtained by solving:

$$\mathbf{Z}_{i+1}^w = \arg \min_{\mathbf{Z}^w} \frac{1}{2} \|\mathbf{Z}_i - \mathbf{Z}^w\|_F^2 + \gamma \alpha \|\mathbf{Z}^w\|_*, \quad (13)$$

where  $\|\cdot\|_F$  is the Frobenius norm, and  $\mathbf{Z}_i$  plays the role of  $\mathbf{u}_i$  in (12),

$$\mathbf{Z}_i = \mathbf{Z}_i^w - \alpha \mathcal{A}^*(\mathcal{A}(\mathbf{Z}_i^w) - \mathbf{y}). \quad (14)$$

A typical condition ensuring convergence of  $\{\mathbf{Z}_i^w\}$  to a minimizer of (10) is to require that  $\alpha \in (0, 1/\|\Phi\|_2^2]$ . Hereafter,  $\|\Phi\|_2$  denotes the spectral norm of matrix  $\Phi$  (i.e., maximum singular value of the matrix).

The task now is to solve the relaxed rank-minimization problem (13). In this paper, Problem (13) is solved efficiently using the *singular value soft-thresholding* (SVT) technique, which provides a closed-form solution by the following theorem [25, 26]:

**Theorem 1** For each  $\tau \geq 0$  and  $\mathbf{Z} \in \mathbb{C}^{M \times N}$ , the SVT operator  $\mathcal{S}_\tau(\mathbf{Z})$  obeys

$$\mathcal{S}_\tau(\mathbf{Z}) = \arg \min_{\mathbf{Z}^w} \frac{1}{2} \|\mathbf{Z} - \mathbf{Z}^w\|_F^2 + \tau \|\mathbf{Z}^w\|_*. \quad (15)$$

Theorem 1 is proved based on the concept of proximal gradient operator of convex functions (here the nuclear-norm). In (15), the SVT operator  $\mathcal{S}_\tau(\mathbf{Z})$  is a nonlinear function which applies a soft-thresholding at level  $\tau$  to the singular values of the input matrix  $\mathbf{Z}$ . Defining a standard elementwise soft-thresholding operator,

$$\mathcal{T}_\tau(x) = \text{sgn}(x) \max(|x| - \tau, 0) = \frac{x}{|x|} \max(|x| - \tau, 0), \quad (16)$$

the SVT operator is computed as

$$\mathcal{S}_\tau(\mathbf{Z}) = \mathbf{U} \mathcal{T}_\tau(\mathbf{\Lambda}) \mathbf{V}^H, \quad (17)$$

where  $\mathbf{Z} = \mathbf{U} \mathbf{\Lambda} \mathbf{V}^H$  is the SVD of  $\mathbf{Z}$ . Note that when applied to vectors or matrices, the soft-thresholding operator  $\mathcal{T}_\tau(\cdot)$  performs entrywise. Using Theorem 1, the solution to Problem (13) is given by

$$\mathbf{Z}_{i+1}^w = \mathcal{S}_{\gamma\alpha}(\mathbf{Z}_i). \quad (18)$$

The iterative steps for solving Problem (10) are provided in Algorithm 1. This algorithm takes an input measurement set  $\mathbf{y}$ , the

parameters  $\alpha$ ,  $\gamma$ , and a predefined tolerance  $\text{tol}$ . The parameter  $\alpha$  is regarded as a gradient stepsize and set to the largest possible value for accelerated convergence, whereas the regularization parameter  $\gamma$  is problem-dependent and needs to be tuned appropriately. In the processing steps, this algorithm performs a gradient evaluation (Step 2) and uses the resultant matrix as input for wall clutter estimation (Step 3) via SVT technique. The algorithm stops when it converges to a local optimum. In practice, the algorithm terminates when the relative change of the objective function becomes negligible (Step 4).

**Algorithm 1:** Proximal gradient iterative estimations of wall clutter in compressive TWRI.

- 
- 1) Initialization: Set  $\mathbf{Z}_0^w \leftarrow \mathcal{A}^*(\mathbf{y})$ , and  $i \leftarrow 0$ .
  - 2) Perform gradient splitting using (14):  
 $\mathbf{Z}_i \leftarrow \mathbf{Z}_i^w - \alpha \mathcal{A}^*(\mathcal{A}(\mathbf{Z}_i^w) - \mathbf{y})$ .
  - 3) Estimate wall component using (18):  
 $\mathbf{Z}_{i+1}^w \leftarrow \mathcal{S}_{\alpha\gamma}(\mathbf{Z}_i)$ .
  - 4) Evaluate the cost function  $f(\mathbf{Z}_{i+1}^w)$  using (10).  
 If  $\frac{|f(\mathbf{Z}_{i+1}^w) - f(\mathbf{Z}_i^w)|}{|f(\mathbf{Z}_i^w)|} < \text{tol}$  then terminate the algorithm,  
 otherwise increment  $i \leftarrow i + 1$  and go to Step 2.
- 

For image reconstruction, the estimated wall clutter is subtracted from the compressed measurements to obtain the clutter-free data. Let  $\hat{\mathbf{Z}}^w$  denote the estimated clutter matrix as the output of Algorithm 1. From (6), (7), and (8), we can formulate a linear model relating the target measurement vector  $\mathbf{y}^t$  to the target image  $\mathbf{s}$ :

$$\mathbf{y}^t = \mathbf{y} - \Phi \text{vec}(\hat{\mathbf{Z}}^w) = \Phi \Psi \mathbf{s} + \mathbf{v}, \quad (19)$$

where we have defined  $\text{vec}(\mathbf{Z}^t) = \Psi \mathbf{s}$  and  $\Phi \text{vec}(\mathbf{Y}) = \mathbf{v}$ . Now a sparse image of the indoor target  $\mathbf{s}$  is obtained by solving the following  $\ell_1$  minimization:

$$\mathbf{s} = \arg \min_{\mathbf{s}} \frac{1}{2} \|\mathbf{y}^t - \Phi \Psi \mathbf{s}\|_2^2 + \lambda \|\mathbf{s}\|_1. \quad (20)$$

Note that Problem (20) can be solved efficiently using the proximal gradient technique described in (11) and (12). Here, we apply the soft-thresholding operator (16) to the auxiliary variable obtained in a similar manner to (14).

## 4. EXPERIMENTAL RESULTS

This section describes experimental results obtained using electromagnetic data. The datasets were acquired using the XFDTD software<sup>1</sup> with Finite Difference Time Domain technique. Data generation used for experiments is presented in Subsection 4.1, and experimental results are given in Subsection 4.2.

### 4.1. Data generation

Data acquisition was conducted using a stepped-frequency synthetic aperture radar system. A linear antenna array was synthesized by moving the transceiver parallel to a concrete wall with 0.15 m thickness, at a standoff distance of 1 m. The antenna array has 51 elements, with inter-element distance of 0.024 m. The scene is imaged by transceiving a stepped-frequency signal of 1 GHz bandwidth, having 334 steps with a stepsize of 3 MHz. Fig. 1 shows the scene layout containing the front wall and two dihedral targets.

<sup>1</sup>Website: www.remcom.com

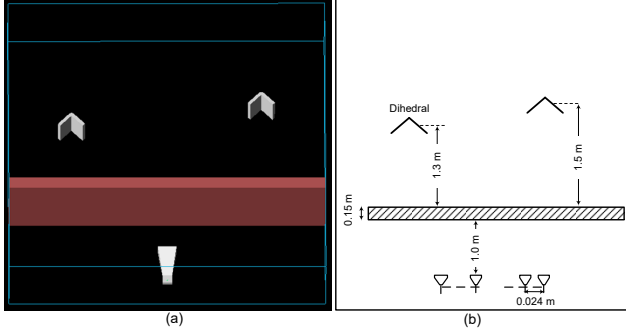


**Fig. 1.** Through-wall radar data collection: (a) geometric scene design, (b) top-view of the indoor scene.

## 4.2. Experimental results

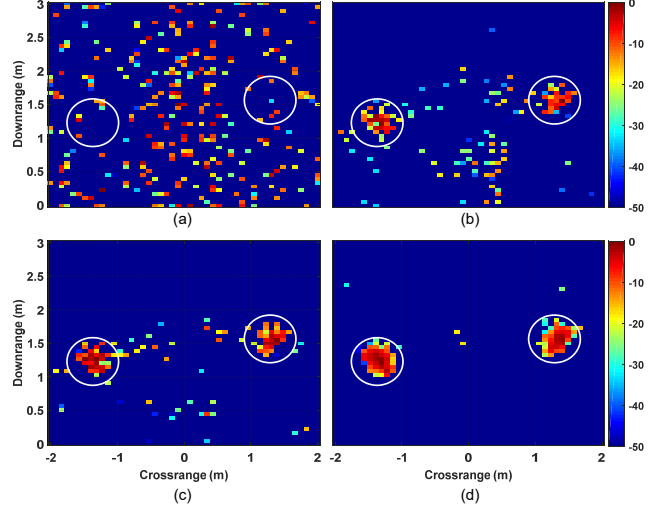
A reduced dataset accounting for only 50% of the full measurements is used for clutter suppression and image formation. The dataset was generated by randomly selecting only 167 (50%) of total frequencies from each antenna locations; the frequency measurements differ across antennas. Input parameters for the LR-MC algorithm are chosen as follows. The gradient stepsize  $\alpha$  is set to  $\alpha = 1/\|\Phi\|_2^2$  for accelerated convergence. The regularization parameter  $\gamma$  is selected as  $\gamma = 10^{-2}\|\mathcal{A}^*(\mathbf{y})\|_2$ . The algorithm is deemed to have converged if the relative change of the objective function is smaller than  $\text{tol} = 10^{-4}$  (see Step 4 in Algorithm 1). For comparison, two-stage approaches, signal estimation followed by wall-clutter mitigation, are implemented on the same dataset. In these two-stage approaches, the missing measurements are first recovered, followed by a SF [5] or a SP technique [6] for wall-clutter mitigation. The target image is formed by solving the  $\ell_1$  minimization problem (20).

Fig. 2 shows the images formed using different clutter mitigation methods. Without clutter removal, strong wall reverberations obscure the targets, making target identification very difficult, as illustrated in Fig. 2(a). Figs. 2(b) and (c) present the images reconstructed after using the two-stage signal estimation followed by SF and SP for clutter reduction, respectively. Although the wall clutter mitigation techniques remove the strong wall reflections, the formed images still contain residual clutter. By contrast, Fig. 2(d) illustrates the image formed after the proposed LR-MC method. It can be observed that the targets are well localized and the clutter is significantly suppressed.

To quantify the performances of the different clutter mitigation methods, the performance measure target-to-clutter ratio (TCR) is used. Let  $A_t$  and  $A_c$  be, respectively, the target and clutter regions of the formed image  $I$ , and let  $N_t$  and  $N_c$  denote, respectively, the number of target and clutter pixels. The TCR (in dB) is defined as

$$\text{TCR} = 10 \log_{10} \left( \frac{\frac{1}{N_t} \sum_{q \in A_t} |I_q|^2}{\frac{1}{N_c} \sum_{q \in A_c} |I_q|^2} \right). \quad (21)$$

Note that the clutter region is considered as the whole image excluding the target region. Table 1 lists the TCRs of the images depicted in Fig. 2. It can be seen that the LR-MC approach yields the highest TCR value (35.56 dB) among the tested clutter mitigation techniques.



**Fig. 2.** Images reconstructed using different wall-clutter mitigation techniques with 50% of the total measurements: (a) without clutter mitigation, (b) two-stage signal estimation & spatial filtering, (c) two-stage signal estimation & subspace projection, and (d) proposed LR-MC approach.

**Table 1.** TCR of the images reconstructed after applying different clutter mitigation approaches using 50% data measurements.

Wall clutter mitigation method	TCR (dB)
Proposed low-rank matrix completion method	<b>35.56</b>
Two-stage signal estimation & subspace projection	24.11
Two-stage signal estimation & spatial filtering	21.49
Without clutter mitigation	-4.02

## 5. CONCLUSION

This paper presented a low-rank matrix completion approach for removing wall clutter in compressive TWRI. The task of wall-clutter mitigation is formulated as a nuclear-norm regularized least squares minimization problem. An iterative algorithm based on the proximal gradient technique is developed to solve the minimization problem, capturing the wall reflections. Experimental results using simulated EM radar data have confirmed the effectiveness of the proposed approach. It mitigates wall reflections in the presence of missing measurements. The proposed LR-MC model is more robust than the existing two-stage wall clutter mitigation methods in a CS context; the LR-MC model estimates the wall clutter more precisely and enhances the quality of indoor image reconstruction.

## Acknowledgments

The work of A. Bouzerdoum and S. L. Phung was supported by a grant from the Australian Research Council (ARC). The work of V. H. Tang was supported by the Vietnam National Foundation for Science and Technology Development (NAFOSTED) under Grant 102.01-2017.307.

## 6. REFERENCES

- [1] M. G. Amin (Ed.), *Through-The-Wall Radar Imaging*. Boca Raton, FL: CRC Press, 2010.
- [2] C. H. Seng, A. Bouzerdoum, M. G. Amin, and S. L. Phung, "Probabilistic fuzzy image fusion approach for radar through wall sensing," *IEEE Trans. Image Processing*, vol. 22, no. 12, pp. 4938–4951, Dec. 2013.
- [3] V. H. Tang, A. Bouzerdoum, and S. L. Phung, "Two-stage through-the-wall radar image formation using compressive sensing," *Journal of Electronic Imaging*, vol. 22, no. 2, pp. 021 006.1–021 006.10, Apr.–Jun. 2013.
- [4] V. H. Tang, A. Bouzerdoum, and S. L. Phung, "Multipolarization through-wall radar imaging using low-rank and jointly-sparse representations," *IEEE Trans. Image Processing*, vol. 27, no. 4, pp. 1763–1776, Apr. 2018.
- [5] Y.-S. Yoon and M. G. Amin, "Spatial filtering for wall-clutter mitigation in through-the-wall radar imaging," *IEEE Trans. Geoscience and Remote Sensing*, vol. 47, no. 9, pp. 3192–3208, Sept. 2009.
- [6] F. H. C. Tivive, A. Bouzerdoum, and M. G. Amin, "A subspace projection approach for wall clutter mitigation in through-the-wall radar imaging," *IEEE Trans. Geoscience and Remote Sensing*, vol. 53, no. 4, pp. 2108–2122, Apr. 2015.
- [7] V. H. Tang, A. Bouzerdoum, and S. L. Phung, and F. H. C. Tivive, "A sparse Bayesian learning approach for through-wall radar imaging of stationary targets," *IEEE Trans. Aerospace and Electronic Systems*, vol. 53, no. 5, pp. 2485–2501, Oct. 2017.
- [8] Y.-S. Yoon and M. G. Amin, "Compressed sensing technique for high-resolution radar imaging," in *Proc. SPIE: Signal Processing, Sensor Fusion, and Target Recognition XVII*, Orlando, FL, Mar. 2008, pp. 69 681A–1–69 681A–10.
- [9] Q. Huang, L. Qu, B. Wu, and G. Fang, "UWB through-wall imaging based on compressive sensing," *IEEE Trans. Geoscience and Remote Sensing*, vol. 48, no. 3, pp. 1408–1415, Mar. 2010.
- [10] J. Yang, A. Bouzerdoum, F. H. C. Tivive, and M. G. Amin, "Multiple-measurement vector model and its application to through-the-wall radar imaging," *Proc. IEEE Int. Conf. Acoustics, Speech and Signal Processing*, pp. 2672–2675, Prague, Czech Republic, 22–27 May 2011.
- [11] V. H. Tang, A. Bouzerdoum, S. L. Phung, and F. H. C. Tivive, "Enhanced through-the-wall radar imaging using Bayesian compressive sensing," in *Proc. SPIE compressive sensing II*, vol. 8717, 2013, pp. 87 170I.1–87 170I.12.
- [12] D. L. Donoho, "Compressed sensing," *IEEE Trans. Information Theory*, vol. 52, no. 4, pp. 1289–1306, Apr. 2006.
- [13] E. J. Candes, J. Romberg, and T. Tao, "Stable signal recovery from incomplete and inaccurate measurements," *Communications on Pure and Applied Mathematics*, vol. 59, no. 8, pp. 1207–1223, Aug. 2006.
- [14] E. Lagunas, M. G. Amin, F. Ahmad, and M. Najar, "Joint wall mitigation and compressive sensing for indoor image reconstruction," *IEEE Trans. Geoscience and Remote Sensing*, vol. 51, no. 2, pp. 891 – 906, Feb. 2013.
- [15] V. H. Tang, A. Bouzerdoum, S. L. Phung, and F. H. C. Tivive, "Enhanced wall clutter mitigation for through-the-wall radar imaging using joint Bayesian sparse signal recovery," *Proc. IEEE Int. Conf. Acoustics, Speech and Signal Processing*, pp. 7804–7808, Florence, Italy, 4–9 May 2014.
- [16] F. Ahmad, J. Qian, and M. G. Amin, "Wall clutter mitigation using discrete prolate spheroidal sequences for sparse reconstruction of indoor stationary scenes," *IEEE Trans. Geoscience and Remote Sensing*, vol. 53, no. 3, pp. 1549–1557, March 2015.
- [17] F. H. C. Tivive, A. Bouzerdoum, and V. H. Tang, "Multi-stage compressed sensing and wall clutter mitigation for through-the-wall radar image formation," in *Proc. IEEE Sensor Array and Multichannel Signal Processing*, Coruna, Spain, Jun. 2014, pp. 489–492.
- [18] V. H. Tang, A. Bouzerdoum, S. L. Phung, and F. H. C. Tivive, "Radar imaging of stationary indoor targets using joint low-rank and sparsity constraints," in *IEEE Int. Conf. Acoustics, Speech and Signal Processing*, Shanghai China, Mar. 2016, pp. 1412–1416.
- [19] V. H. Tang, A. Bouzerdoum, S. L. Phung, and F. H. C. Tivive, "Indoor scene reconstruction for through-the-wall radar imaging using low-rank and sparsity constraints," in *IEEE Radar Conference*, PA, USA, May 2016, pp. 1–4.
- [20] B. Recht, M. Fazel, and P. A. Parrilo, "Guaranteed minimum-rank solutions of linear matrix equations via nuclear norm minimization," *SIAM Rev.*, vol. 52, no. 3, pp. 471–501, Aug. 2010.
- [21] P. L. Combettes and V. R. Wajs, "Signal recovery by proximal forward-backward splitting," *SIAM Journal of Multiscale Modeling Simulation*, vol. 4, no. 4, pp. 1168–1200, Nov. 2006.
- [22] C. Vonesch and M. Unser, "A fast thresholded Landweber algorithm for wavelet-regularized multidimensional deconvolution," *IEEE Trans. Image Processing*, vol. 17, no. 4, pp. 539–549, April 2008.
- [23] A. Beck and M. Teboulle, "A fast iterative shrinkage-thresholding algorithm for linear inverse problems," *SIAM Journal on Imaging Sciences*, vol. 2, no. 1, pp. 183–202, March 2009.
- [24] S. J. Wright, R. D. Nowak, and M. A. T. Figueiredo, "Sparse reconstruction by separable approximation," *IEEE Trans. Signal Processing*, vol. 57, no. 7, pp. 2479–2493, July 2009.
- [25] S. Ma, D. Goldfarb, and L. Chen, "Fixed point and Bregman iterative methods for matrix rank minimization," *Mathematical Programming*, vol. 128, no. 1, pp. 321–353, Jun. 2011.
- [26] J.-F. Cai, E. J. Candes, and Z. Shen, "A singular value thresholding algorithm for matrix completion," *SIAM Journal on Optimization*, vol. 20, no. 4, pp. 1956–1982, Mar. 2010.